

Blind spectral unmixing to identify molecular signatures of absorbers in multispectral optoacoustic tomography

Stefan Morscher, Jürgen Glatz, Nikolaos C. Deliolanis*, Andreas Buehler, Daniel Razansky and Vasilis Ntziachristos

Chair for Biological Imaging & Institute for Biological and Medical Imaging
Technische Universität München & Helmholtz Zentrum München, Munich, Germany

ABSTRACT

Multispectral optoacoustic (photoacoustic) tomography (MSOT) exploits the high resolutions provided by ultrasound imaging technology in combination with the more biologically relevant optical absorption contrast. Traces of molecules with different spectral absorption profiles, such as blood (oxy- and de-oxygenated) and biomarkers can be recovered using multiple wavelengths excitation and a set of methods described in this work. Three unmixing methods are examined for their performance in decomposing images into components in order to locate fluorescent contrast agents in deep tissue in mice. Following earlier works we find Independent Component Analysis (ICA), which relies on the strong criterion of statistical independence of components, as the most promising approach, being able to clearly identify concentrations that other approaches fail to see. The results are verified by cryosectioning and fluorescence imaging.

Keywords: Photoacoustic tomography, Multispectral Imaging, Spectral unmixing, Blind deconvolution, Independent component analysis, Fluorescence, Molecular Imaging

1. INTRODUCTION

Opto-acoustic (or photoacoustic) imaging for microscopic applications began to evolve in the 80's^{1,2}. The application of the underlying effects for tomographic approaches has recently gained momentum in research as it offers ultrasound resolution with imaging depths given by near infrared laser penetration. The contrast in the images is generated mainly by intrinsic optical absorption^{3,4}. Usage of ultrasound detector arrays recently rendered mechanical movement of the detector unnecessary⁵, thus allowing for image generation at much higher speeds even enabling video rate imaging⁶.

Utilizing the advantages of specific optical absorption contrast along different excitation wavelengths enables differential imaging of the bio-distribution of vasculature⁷, blood oxygen saturation⁸ and biomarkers⁹⁻¹². Especially hemoglobin in blood still has a high optical absorption in the near infrared wavelengths with respect to other absorbers present in biological tissue – and thus generates a large photoacoustic signal. This renders larger vascular structures visible in the reconstructed photoacoustic images without any additional tools or methods. For contrast agents used in biological applications the concentration of absorbing molecules that biologically accumulate in targeted tissue (e.g. tumors) is lower, thus generating a weaker opto-acoustic signal that is usually not distinguishable from the background when inspecting the images with the bare eye alone. To a large extent this arises from the aforementioned high optical density of blood that accounts for large parts of the intrinsic contrast in the image and makes the use of advanced methods and tools necessary in order to visualize the spatial distribution of less optically dense substances. The acquisition of multispectral measurements and the use of blind spectral unmixing methods has improved the performance in optical biomedical imaging, mainly in fluorescence¹³⁻¹⁵ and, recently, in optoacoustic imaging¹⁶. Herein, we present the results from MSOT experiments imaging fluorochromes in deep tissue and examine the performance of three different spectral unmixing methods.

*email: ndeliolanis@yahoo.com

2. METHODS

1.1 Experiment

Image acquisition was performed using the setup previously described in Ref. 6. Illumination is provided by a tunable wavelength OPO laser (Opotek, Inc. Carlsbad, CA) that delivers 10 pulses per seconds with a duration of < 10 ns each. The generated opto-acoustic signals are detected by a 64-element ultrasonic transducer array with a center frequency of 5 Mhz covering an angle of 172° (Imasonic SaS, Voray, France). Image reconstruction of all acquired single wavelength images is done using a model-based inversion algorithm¹⁷, where the signals were averaged over 25 acquisition cycles. The laser was tuned from 690 nm to 835 nm in steps of 5 nm, so a total number of 30 wavelengths were recorded in the measurements. In order to verify the results achieved by the spectral unmixing the sample was imaged in a cryoslicing and epi-illumination imaging system¹⁸ that is able to visualize even small concentrations of fluorescent contrast agents in tissue.

In order to compare the performance of the techniques detailed below, a solid inclusion was created in the esophagus of a number of dead CD1 mice. The inclusion is made up of agar and Cy7 (GE Healthcare) as a fluorescent dye that has a distinct absorption spectrum with a peak at 750nm (see absorption spectrum in Fig 4b). The concentration of the contrast agent was varied in order to study the performance of the unmixing with different concentrations. In order to create the inclusions in esophagus and stomach a tubing was inserted from the mouth and the agar based solution was injected to fill up all vacant space. The neck region was chosen as the imaging plane due to relatively small diameter and few highly absorbing structures in the tissue that possibly interfere with the signal of the inclusion. After imaging the mice with the MSOT system the location and nature of the inclusion was verified using the aforementioned cryoslicing tool that detects fluorescence in the desired locations.

1.2 Unmixing

In order to spectrally unmix and decompose the reconstructed optoacoustic images into image components that identify the biodistribution of substances that give spectral contrast, three different approaches were examined and are described below. Generally speaking, the term unmixing means finding a solution for the unknown right hand side of the equation

$$M = WS,$$

where M is the measured data $m \times n$ array that consists of measurements at m different wavelengths, each containing a total of n pixels. The number of sources or components the acquired images are to be split into is c and usually equals m . Components are characterized by their distinct absorption spectrum across the measured wavelengths in the weighting $m \times c$ matrix W , and their spatial distribution in the $c \times n$ matrix S . In order to maintain algebraic correctness the residual error is to be minimized so that the original data can be re-mixed using the resulting matrices.

Spectral fitting is a simple and straightforward approach to pursue spectral unmixing using a set of measured absorption spectra of components contained in the measured sample. The spectra in W are inverted by means of the Moore-Penrose inverse^{19,20} and multiplied from the right with the measurements in M to extract the sources S . A number of other, more complex algorithms for matrix factorization and multivariate data analysis have been suggested in literature²¹⁻²³.

Other approaches do not use any a-priori knowledge and are thus referred to as “Blind Source Separation”. Instead of known spectra they use constraints that are implied in the measured data to enable splitting information into two parts that in this case contain spectra and component information. Two of the most promising methods in this field are Principal Component Analysis (PCA)²³ and Independent Component Analysis (ICA)²², where both apply statistical constraints to the separation of the measured datasets.

PCA on the one hand decomposes data into components that are statistically uncorrelated and thus orthogonal. This can be mathematically computed either by a singular value decomposition or an eigenvalue decomposition of the covariance matrix of the data. Implementations of the algorithm are available for all common computational tools. Components are sorted according to their eigen value (or singular value respectively), which is equivalent to the variance that is represented by the component. Components with smaller variance are ranked lowest and mostly contain noise and can thus often be neglected, additionally promoting PCA as a simple means of noise or dimension reduction in signal preprocessing before the actual step of unmixing.

ICA on the other hand pursues a similar approach based on statistical independence rather than the weaker criterion of uncorrelatedness, thus usually providing more accurate separation results. We use the FastICA algorithm²⁴ in the MATLAB implementation provided on the homepage of the authors. According to the central limit theorem²⁵ a mixture of signals is always more gaussian than the individual signals, so separating measurement data trying to maximize the non-Gaussianity using kurtosis gives a set of statistically independent source components. Because a way to measure the importance of the component is not available with the results from ICA, the components will appear in random order. As this can make evaluation of results tedious and time consuming with an increasing number of wavelengths, an initial guess of the spectral profiles of components expected to be contained in the sample can be supplied to the algorithm to influence the sorting of components.

3. RESULTS AND DISCUSSION

Representative reconstructed images of the mouse with an inclusion with contrast agent concentration of 1cm^{-1} O.D. are displayed in Fig. 1a–c. The signal change due to variable absorption of the inclusion across wavelengths is very small and it is not visible after having applied contrast adjustment and thresholding to the images. This inability demonstrates the necessity of spectral unmixing techniques that are nevertheless able to reveal the contrast agent distribution. Other concentrations of fluorescent dye in the inclusion show similar behaviour in terms of the unmixing and are omitted in the discussion. Presence and location of fluorescence of the dye are clearly identified in the cryosection RGB and fluorescent images (Fig. 2a-b). A fluorescent straw was being added as a reference to quantify the fluorescent signal in the sample.

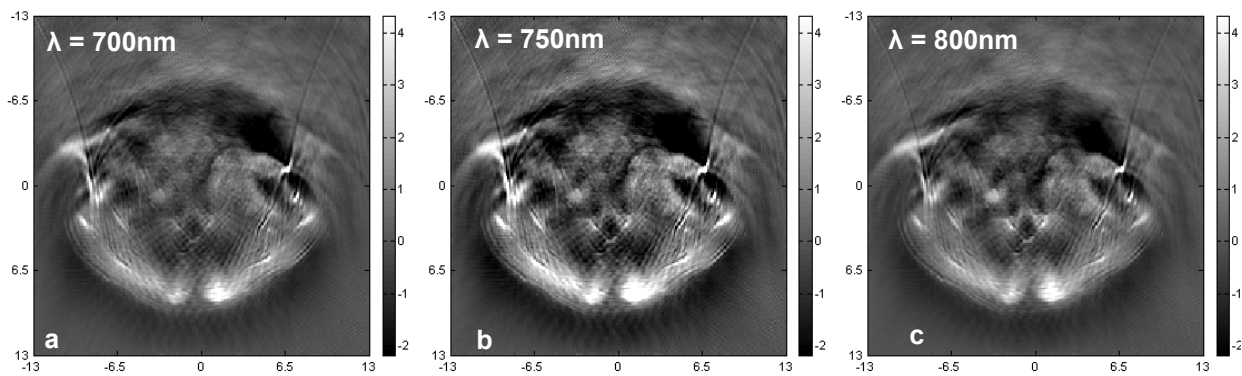


Figure 1. a-c) Representative optoacoustic tomographic reconstructions of the mouse torso at 700nm, 750nm and 800nm respectively, the inclusion is invisible to the bare eye. Contrast enhancement and thresholding are applied to the images

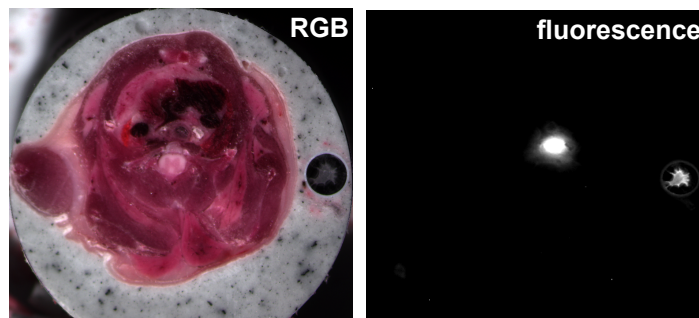


Figure 2. a) RGB Image of Cryosection b) Fluorescence Image of Cryosection

Although spectral fitting proved to be a viable approach for more superficial applications in earlier works¹⁶, it failed to recover a clear image of the inclusion (see Fig. 3a) in deep tissue using the Cy7 spectrum measured by the spectrometer (see Fig. 2a; peak absorption $\mu_a = 2.3 \text{ cm}^{-1}$, 1 cm^{-1} O.D). The main reason is spectral variation of light attenuation in tissue that render the spectral profile of light fluence in deep tissue practically unknown. As a result, the spectral variation of optoacoustic signals does not match with the known absorption spectrum of the fluorochromes used in spectral fitting. Furthermore the strong background absorbers dominate against the comparatively small signal created by the fluorophore in the inclusion and makes it difficult to obtain a clear picture just using means of matrix inversion.

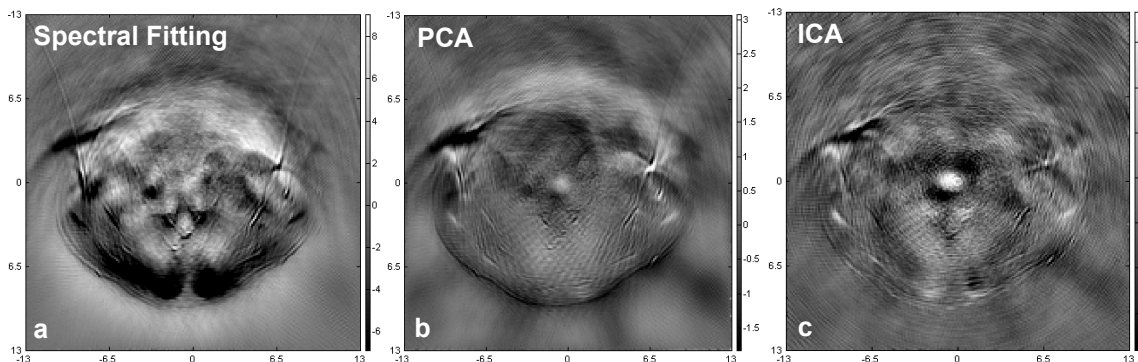


Figure 3. a) Unmixed Images using Spectral Fitting b) PCA and c) ICA.

Processing with PCA produces more promising component images, one of which contains the inclusion. This is possible because the uncorrelatedness is still given at increasing depth and enables separation without prior knowledge of what absorbers are present in the sample. The comparatively poor contrast is due to the fact that the signal generated by the inclusion is not clearly separated from other signals created by strong surface absorbers. For the same reason the corresponding spectrum resulting from the PCA decomposition is not decisive and thus does not provide a mean to identify the desired component by recognizing its spectral behaviour. Identifying the desired component (see Fig 3b) by looking at the component images was possible in this case, but the spatial distribution is expected to be unknown in many applications. Even though PCA decomposes a set of cross-wavelength images into the same amount of components, in general only few of the components actually contain recognizable structures, whilst the others only contain noise and artifacts.

Finally, unmixing with ICA delivers best performance with the inclusion being well isolated (Fig. 3c). The superior performance is caused by the fact that the underlying criterion of statistical independence of the components is stronger than the uncorrelatedness criterion used by PCA and thus results in superior separation abilities. This creates a larger variety of non-noise components with more decisive spectra. It can be observed in Fig. 4b that the spectrum recovered by ICA (dotted line) has a shifted absorption peak compared to the spectrometer measurements (solid line). This blue-shift is attributed to the spectrally dependent drop of light fluence in deep tissue. In ex-vivo tissue the dominant absorber is de-oxygenated hemoglobin (absorption spectrum depicted in Figure 4a) whose local absorption peak at 760nm reduces illumination intensity in the deep location of the inclusion and so shifts the peak of the discovered component. For the fact that the used implementation is based on an iterative algorithm the measured spectrometer absorption spectrum can be supplied to the algorithm as an initial guess despite the occurrence of the blue-shift and the algorithm still converges to the correct solution and the true deep tissue spectrum depicted in Fig 4b. Using the initial guess allows for a more automated detection of certain absorbers, without the need to visually inspect many components to identify the relevant ones.

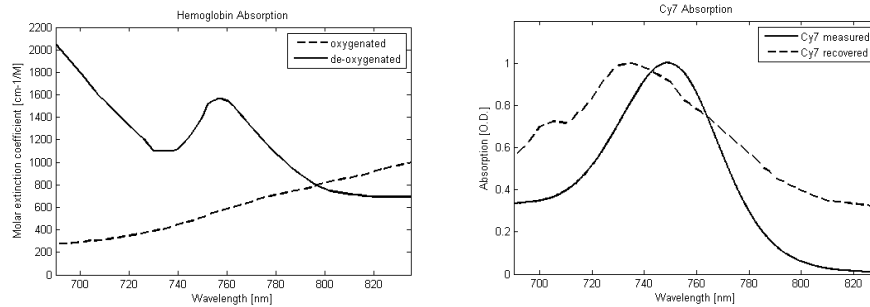


Figure 4. a) Hemoglobin Absorption b) Cy7 Absorption as measured in the spectrometer and as recovered by ICA.

4. CONCLUSION

Optoacoustic tomography is emerging as a high resolution deep tissue biomedical imaging method and especially multispectral acquisitions can serve to identify the biodistribution of various absorbers. Post-processing of the data requires a robust spectral unmixing algorithm and blind unmixing with ICA is shown to perform best, boosting the detection sensitivity of MSOT beyond the limits of differential or fitting-based unmixing methods. The main advantage lies in the ability to separate measurement data without a-priori knowledge about the sources present in the sample. Still, if knowledge is available, the process can be simplified by supplying spectra of absorbers known to be present in the sample as an initial guess and thus guiding the algorithm.

REFERENCES

- [1] Rosenwaig, A., "Potential clinical applications of photoacoustics," *Clin Chem*, 28(9), 1878-1881 (1982).
- [2] Busse, G., and Rosenwaig, A., "Subsurface imaging with photoacoustics," *Appl. Phys. Lett.*, 36(10), 815-816 (1980).
- [3] Wang, X. D., Pang, Y. J., Ku, G. *et al.*, "Noninvasive laser-induced photoacoustic tomography for structural and functional in vivo imaging of the brain," *Nature Biotechnology*, 21(7), 803-806 (2003).
- [4] Zhang, H. F., Maslov, K., Stoica, G., and Wang, L. H. V., "Functional photoacoustic microscopy for high-resolution and noninvasive in vivo imaging," *Nature Biotechnology*, 24(7), 848-851 (2006).
- [5] Brecht, H. P., Su, R., Fronheiser, M. *et al.*, "Whole-body three-dimensional optoacoustic tomography system for small animals," *Journal of Biomedical Optics*, 14, 064007 (2009).
- [6] Buehler, A., Herzog, E., Razansky, D., and Ntziachristos, V., "Video rate optoacoustic tomography of mouse kidney perfusion," *Opt. Lett.*, 35(14), 2475-2477 (2010).
- [7] Hoelen, C. G. A., de Mul, F. F. M., Pongers, R., and Dekker, A., "Three-dimensional photoacoustic imaging of blood vessels in tissue," *Opt. Lett.*, 23(8), 648-650 (1998).
- [8] Wang, X., Xie, X., Ku, G., Wang, L. V., and Stoica, G., "Noninvasive imaging of hemoglobin concentration and oxygenation in the rat brain using high-resolution photoacoustic tomography," *J Biomed Opt*, 11(2), 024015 (2006).
- [9] Ntziachristos, V., and Razansky, D., "Molecular imaging by means of multispectral optoacoustic tomography (MSOT)," *Chemical Reviews*, 110(5), 2783-2794 (2010).
- [10] Taruttis, A., Herzog, E., Razansky, D., and Ntziachristos, V., "Real-time imaging of cardiovascular dynamics and circulating gold nanorods with multispectral optoacoustic tomography," *Opt. Express*, 18(19), 19592-19602 (2010).
- [11] Li, P.-C., Wang, C.-R. C., Shieh, D.-B. *et al.*, "In vivo photoacoustic molecular imaging with simultaneous multiple selective targeting using antibody-conjugated gold nanorods," *Opt. Express*, 16(23), 18605-18615 (2008).
- [12] Razansky, D., Distel, M., Vinegoni, C. *et al.*, "Multispectral opto-acoustic tomography of deep-seated fluorescent proteins in vivo," *Nature Photonics*, 3(7), 412-417 (2009).

- [13] Hillman, E. M. C., and Moore, A., "All-optical anatomical co-registration for molecular imaging of small animals using dynamic contrast," *Nat Photon*, 1(9), 526-530 (2007).
- [14] Xu, H., and Rice, B. W., "In-vivo fluorescence imaging with a multivariate curve resolution spectral unmixing technique," *Journal of Biomedical Optics*, 14(6), 064011-9 (2009).
- [15] Montcuquet, A.-S., Herve, L., Navarro, F., Dinten, J.-M., and Mars, J. I., "Nonnegative matrix factorization: a blind spectra separation method for in vivo fluorescent optical imaging," *Journal of Biomedical Optics*, 15(5), 056009-14 (2010).
- [16] Glatz, J., Deliolanis, N. C., Buehler, A., Razansky, D., and Ntziachristos, V., "Blind source unmixing in multi-spectral optoacoustic tomography," *Opt. Express*, 19(4), 3175-3184 (2011).
- [17] Rosenthal, A., Razansky, D., and Ntziachristos, V., "Quantitative optoacoustic signal extraction using sparse signal representation," *IEEE Transactions on Medical Imaging*, 28(12), 1997-2006 (2009).
- [18] Sarantopoulos, A., Themelis, G., and Ntziachristos, V., "Imaging the Bio-Distribution of Fluorescent Probes Using Multispectral Epi-Illumination Cryoslicing Imaging," *Molecular Imaging and Biology*, DOI: 10.1007/s11307-010-0416-8
- [19] Moore, E., "On the reciprocal of the general algebraic matrix," *Bulletin of the American Mathematical Society*, 26, 394-395 (1920).
- [20] Penrose, R., "A generalized inverse for matrices," *Proceedings of the Cambridge Philosophical Society*, 51, 406-412 (1955).
- [21] Cichocki, A., Zdunek, R., Phan, A. H., and Amari, S.-i., [Nonnegative Matrix and Tensor Factorizations: Applications to Exploratory Multi-way Data Analysis and Blind Source Separation] Wiley, (2009).
- [22] Hyvärinen, A., Karhunen, J., and Oja, E., [Independent Component Analysis, Adaptive and Learning Systems for Signal Processing, Communications, and Control] Wiley InterScience, (2002).
- [23] Jolliffe, I. T., [Principal Component Analysis] Springer, (2002).
- [24] Hyvarinen, A., "Fast and robust fixed-point algorithms for independent component analysis," *Ieee Transactions on Neural Networks*, 10(3), 626-634 (1999).
- [25] Le Cam, L., "The Central Limit Theorem Around 1935," *Statistical Science*, 1(1), 78-91 (1986).